

From Equilibrium to Transport Properties of Strongly Correlated Fermi Liquids

Thomas Schäfer

*Department of Physics, North Carolina State University,
Raleigh, NC 27695*

We summarize recent results regarding the equilibrium and non-equilibrium behavior of cold dilute atomic gases in the limit in which the two body scattering length a goes to infinity. In this limit the system is described by a Galilean invariant (non-relativistic) conformal field theory. We discuss the low energy effective lagrangian appropriate to the limit $a \rightarrow \infty$, and compute low energy coefficients using an ϵ -expansion. We also show how to combine the effective lagrangian with kinetic theory in order to compute the shear viscosity, and compare the kinetic theory predictions to experimental results extracted from the damping of collective modes in trapped Fermi gases.

Keywords: cold atomic gases, conformal symmetry, shear viscosity

1. Introduction

Over the last ten years there has been remarkable progress in the study of “designer fluids”, dilute, non-relativistic Bose and Fermi gases in which the scattering length between the Bosons or Fermions can be continuously adjusted. In the following we are particularly interested in Fermi gases, since these systems are stable for both positive and negative values of the scattering length, including the strongly correlated limit in which the scattering length is taken to infinity.

The scattering length is controlled through a Feshbach resonance. Alkali atoms such as ^6Li and ^{40}K have a single valence electron. When a dilute gas of atoms is cooled to very low temperatures, we can view the atoms as pointlike particles interacting via interatomic potentials which depend on the hyperfine quantum numbers. A Feshbach resonance arises if a molecular bound state in a “closed” hyperfine channel crosses near the threshold of an energetically lower “open” channel. Because the magnetic moments of the open and closed states are in general different, Feshbach resonances can be tuned using an applied magnetic field. At resonance the two-body scattering

length in the open channel diverges, and the cross section σ is limited only by unitarity, $\sigma(k) = 4\pi/k^2$ for low momenta k . In the unitarity limit, details about the microscopic interaction are irrelevant, and the system displays universal properties.

Near a Feshbach resonance the scattering length behaves as

$$a = a_0 \left(1 + \frac{\Delta B}{B - B_0} \right) \quad (1)$$

where a_0 is the non-resonant value of the scattering length (typically on the order of the effective range of the interatomic potential), B is the magnetic field, B_0 the position of the resonance, and ΔB the width. A small negative scattering length corresponds to a weak attractive interaction between the atoms. This case is known as the BCS (Bardeen-Cooper-Schrieffer) limit. On the other side of the resonance the scattering length is positive. In the BEC (Bose-Einstein condensation) limit the interaction is strongly attractive and the fermions form deeply bound molecules. For this reason the unitarity limit $a \rightarrow \infty$ is also known as the BCS/BEC crossover.

The unitarity limit is of interest to QCD practitioners for a number of reasons:

- The unitarity limit provides an approximate description of dilute neutron matter. The neutron-neutron scattering length is $a_{nn} = -18$ fm, and the effective range is $r_{nn} = 2.8$ fm. This means that there is a range of densities, relevant to the outer layers of neutron stars, for which the interparticle spacing is large compared to the effective range, but small compared to the scattering length.
- The Fermi gas at unitarity is a high T_c superconductor. There is an attractive interaction in the spin singlet channel which leads to s-wave superconductivity below some critical temperature T_c . In the unitarity limit the only energy scale in the problem is the Fermi energy E_F , and we must have $k_B T_c = \alpha E_F$ with some numerical constant α . Quantum Monte Carlo calculations (and experimental results) indicate that $\alpha \simeq 0.15$ [1,2], much larger than in ordinary (or even high T_c) electronic superconductors, but comparable to what might be achieved in color superconducting quark matter [3].
- The limit $a \rightarrow \infty$ corresponds to a non-relativistic conformal field theory [4]. In the unitarity limit there is no scale in the problem (other than the thermodynamic variables temperature and density). Indeed, one can show that the theory is not only scale invariant, but invariant under the full conformal group. This raises the

question whether there are any physical consequences of conformal symmetry that go beyond results that follow from scale invariance. It also raises the possibility that a holographic description, similar to the *AdS/CFT* correspondence, can be obtained [5,6].

- Non-relativistic fermions at unitarity behave as a very good fluid and show interesting transport properties, including a very small shear viscosity. Kinetic theory suggests that the shear viscosity is inversely proportional to the scattering cross section, and reaches a minimum at unitarity. This expectation is confirmed by experiments that demonstrate large elliptic flow and a very small damping rate for collective oscillations [7,8].

2. Equilibrium Properties

We begin by analyzing equilibrium properties of the dilute Fermi gas at unitarity. If the temperature is large, $k_B T > E_F$, then the scattering cross section is regularized by the thermal wave length, and the effective interaction is weak. Here the Fermi energy is defined by $E_F = (3\pi^2 n)^{2/3}/(2m)$, where n is the density, and m is the mass of the atoms. In the high temperature regime the equation of state is well described by the Virial expansion, and the system has single particle excitations with the quantum numbers of the fundamental fermions. In the regime $k_B T \sim E_F$ the interactions are strong. As noted above, superfluidity occurs at $k_B T_c \simeq 0.15 E_F$. Below the critical temperature the excitations are Goldstone bosons. In following section we will discuss the effective theory of the Goldstone bosons, and relate the parameters in the effective lagrangian to static properties of the system.

2.1. Low Energy Effective Theory and Density Functional

The Goldstone boson field can be defined as the phase of the difermion condensate $\langle \psi\psi \rangle = e^{2i\varphi} |\langle \psi\psi \rangle|$. The effective Lagrangian at next-to-leading order (NLO) in derivatives of φ and the external potential is [9]

$$\mathcal{L} = c_0 m^{3/2} X^{5/2} + c_1 m^{1/2} \frac{(\vec{\nabla} X)^2}{\sqrt{X}} + \frac{c_2}{\sqrt{m}} \left[(\nabla^2 \varphi)^2 - 9m \nabla^2 V \right] \sqrt{X}, \quad (2)$$

where we have defined

$$X = \mu - V - \dot{\varphi} - \frac{(\vec{\nabla} \varphi)^2}{2m}. \quad (3)$$

Here, μ is the chemical potential and $V(\vec{x}, t)$ is an external potential. The functional form of the effective lagrangian is fixed by the symmetries of

the problem, Galilean invariance, $U(1)$ symmetry, and conformal symmetry. The NLO effective lagrangian is characterized by three dimensionless parameters, c_0, c_1, c_2 . These parameters can be related to physical properties of the system. The first parameter, c_0 , can be related to the equation of state. We have

$$c_0 = \frac{2^{5/2}}{15\pi^2\xi^{3/2}}, \quad (4)$$

where ξ determines the chemical potential in units of the Fermi energy, $\mu = \xi E_F$. The two NLO parameters c_1, c_2 are related to the momentum dependence of correlation functions. The phonon dispersion relation, for example, is given by

$$q_0 = v_s q \left[1 - \pi^2 \sqrt{2\xi} \left(c_1 + \frac{3}{2} c_2 \right) \frac{q^2}{k_F^2} + O(q^4 \log(q^2)) \right] \quad (5)$$

where $v_s = \sqrt{\xi/3} v_F$ and $v_F = k_F/m$. The static susceptibility

$$\chi(q) = -i \int dt d^3x e^{-i\vec{q}\cdot\vec{x}} \langle \psi^\dagger \psi(0) \psi^\dagger \psi(x) \rangle \quad (6)$$

involves a different linear combination of c_1 and c_2 ,

$$\chi(q) = -\frac{mk_F}{\pi^2\xi} \left[1 + 2\pi^2 \sqrt{2\xi} \left(c_1 - \frac{9}{2} c_2 \right) \frac{q^2}{k_F^2} + O(q^4 \log(q^2)) \right]. \quad (7)$$

Higher derivative terms in the effective lagrangian can also be used to compute the energy of inhomogeneous matter. At NLO in an expansion in derivatives of the density we find the following energy density functional [10]

$$\begin{aligned} \mathcal{E}(x) = n(x)V(x) + \frac{3 \cdot 2^{2/3}}{5^{5/3} m c_0^{2/3}} n(x)^{5/3} - \frac{4}{45} \frac{2c_1 + 9c_2}{m c_0} \frac{(\nabla n(x))^2}{n(x)} \\ - \frac{12}{5} \frac{c_2}{m c_0} \nabla^2 n(x). \end{aligned} \quad (8)$$

The first two terms correspond to the local density approximation (LDA) and the terms proportional to c_1 and c_2 are the leading correction to the LDA involving derivatives of the density.

2.2. Epsilon Expansion

At unitarity the determination of c_1 and c_2 is a non-perturbative problem, and we will perform the calculation using an expansion around $d = 4 - \epsilon$ spatial dimensions [11,12]. Our starting point is the lagrangian

$$\mathcal{L} = \Psi^\dagger \left[i\partial_0 + \sigma_3 \frac{\vec{\nabla}^2}{2m} \right] \Psi + \mu \Psi^\dagger \sigma_3 \Psi + (\Psi^\dagger \sigma_+ \Psi \phi + h.c.) - \frac{1}{C_0} \phi^\dagger \phi, \quad (9)$$

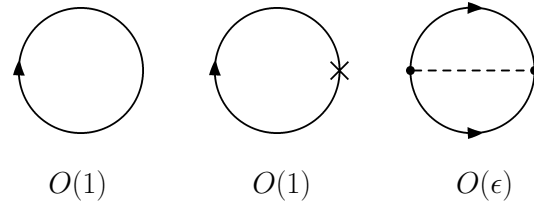


Fig. 1. Leading order contributions to the effective potential in the epsilon expansion. Solid lines denote fermions propagators, dashed lines denote boson propagators, and the cross is an insertion of the chemical potential.

where $\Psi = (\psi_\uparrow, \psi_\downarrow)^T$ is a two-component Nambu-Gorkov field, σ_i are Pauli matrices acting in the Nambu-Gorkov space, $\sigma_\pm = (\sigma_1 \pm i\sigma_2)/2$, ϕ is a complex boson field, and C_0 is a coupling constant. In dimensional regularization the fermion-fermion scattering length becomes infinite for $1/C_0 \rightarrow 0$.

The epsilon expansion is based on the observation that the fermion-fermion scattering amplitude near $d = 4$ dimensions is saturated by the propagator of a boson with mass $2m$. The coupling of the boson to pairs of fermions is given by

$$g = \frac{\sqrt{8\pi^2\epsilon}}{m} \left(\frac{m\phi_0}{2\pi} \right)^{\epsilon/4}. \quad (10)$$

In the superfluid phase ϕ acquires an expectation value $\phi_0 = \langle \phi \rangle$. We write the boson field as $\phi = \phi_0 + g\varphi$. The lagrangian is split into a free part

$$\mathcal{L}_0 = \Psi^\dagger \left[i\partial_0 + \sigma_3 \frac{\vec{\nabla}^2}{2m} + \phi_0(\sigma_+ + \sigma_-) \right] \Psi + \varphi^\dagger \left(i\partial_0 + \frac{\vec{\nabla}^2}{4m} \right) \varphi, \quad (11)$$

and an interacting part $\mathcal{L}_I + \mathcal{L}_{ct}$, where

$$\mathcal{L}_I = g (\Psi^\dagger \sigma_+ \Psi \varphi + h.c.) + \mu \Psi^\dagger \sigma_3 \Psi + 2\mu \varphi^\dagger \varphi, \quad (12)$$

$$\mathcal{L}_{ct} = -\varphi^\dagger \left(i\partial_0 + \frac{\vec{\nabla}^2}{4m} \right) \varphi - 2\mu \varphi^\dagger \varphi. \quad (13)$$

Note that the leading self energy corrections to the boson propagator generated by the interaction term \mathcal{L}_I cancel against the counterterms in \mathcal{L}_{ct} . The chemical potential term for the fermions is included in \mathcal{L}_I rather than in \mathcal{L}_0 . This is motivated by the fact that near $d = 4$ the system reduces to a non-interacting Bose gas and $\mu \rightarrow 0$. We will count μ as a quantity of $O(\epsilon)$. The Feynman rules are quite simple. The fermion and boson propagators

$$-\Pi = \left(\begin{array}{cc} \text{---}\times\text{---} & \text{---}\rightarrow\bullet\rightarrow\text{---} \quad \text{---}\rightarrow\bullet\rightarrow\text{---} \\ \text{---}\leftarrow\bullet\leftarrow\text{---} & \text{---}\leftarrow\bullet\leftarrow\text{---} \end{array} \right)$$

Fig. 2. Scalar self energy at LO in the epsilon expansion.

are

$$G(p_0, p) = \frac{i}{p_0^2 - E_p^2} \begin{bmatrix} p_0 + \epsilon_p & -\phi_0 \\ -\phi_0 & p_0 - \epsilon_p \end{bmatrix}, \quad (14)$$

$$D(p_0, p) = \frac{i}{p_0 - \epsilon_p/2}, \quad (15)$$

where $E_p^2 = \epsilon_p^2 + \phi_0^2$ and $\epsilon_p = p^2/(2m)$. The fermion-boson vertices are $ig\sigma^\pm$. Insertions of the chemical potential are $i\mu\sigma_3$. Both g^2 and μ are corrections of order ϵ .

In order to determine c_0, c_1, c_2 we have to compute three physical observables. We have studied $\xi = \mu/E_F$, and the curvature terms in the phonon dispersion relation and the static susceptibility. The universal parameter ξ was originally calculated by Nishida and Son. They computed the effective potential to NLO in the epsilon expansion, see Fig. 1. The derivative of the effective potential with respect to μ determines the density n , and the relation between n and μ fixes ξ . The result is

$$\xi = \frac{\epsilon^{3/2}}{2} \left[1 + \frac{1}{8}\epsilon \log(\epsilon) - \frac{1}{4}(12C - 5 + 5 \log(2))\epsilon + O(\epsilon^2) \right], \quad (16)$$

with $C = 0.144$. The phonon dispersion relation can be extracted from the scalar propagator. We introduce a two-component scalar field $\Phi = (\varphi, \varphi^*)$. The scalar propagator satisfies a Dyson-Schwinger equation [13]

$$\left(\begin{array}{cc} \text{---}\rightarrow\text{---} & \text{---}\leftarrow\text{---} \\ \text{---}\leftarrow\text{---} & \text{---}\rightarrow\text{---} \end{array} \right)^{-1} = \left(\begin{array}{cc} \text{---}\rightarrow\text{---} & \\ & \text{---}\leftarrow\text{---} \end{array} \right)^{-1} - \Pi \quad (17)$$

At LO in the epsilon expansion the self energy is determined by the diagrams shown in Fig. 2. NLO contributions were calculated in [10]. The phonon dispersion relation is

$$p_0 = \sqrt{\mu\epsilon_p} \left(1 + \frac{\epsilon}{8} \right) \left\{ 1 + \frac{\epsilon_p}{8\mu} \left(1 - \frac{\epsilon}{4} \right) + \dots \right\} \quad (18)$$

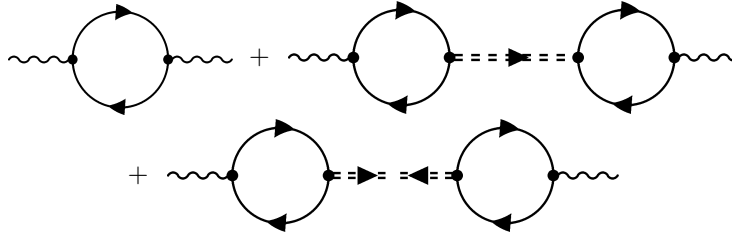


Fig. 3. Leading order contributions to the static susceptibility. The wiggly line denotes an external current. The double line is the scalar propagator defined in equ. (17).

We note that the dispersion relation curves up (unlike ${}^4\text{He}$, but similar to weakly interacting Bose gases). This implies that there is $\varphi \rightarrow \varphi + \varphi$ decay. Finally, we can determine the static susceptibility. Computing the diagrams in Fig. 3 we get [10,14]

$$\chi(q) = -\frac{2Z}{\epsilon\mu} \left\{ 1 - \frac{1}{8} \left(\frac{q^2}{m\mu} \right) \left(1 - \frac{\epsilon}{4} \right) + O(q^4) \right\} \left(\frac{m\phi_0}{2\pi} \right)^{d/2}, \quad (19)$$

$$Z = 1 - \frac{1}{2} (\gamma - \log(2)) \epsilon.$$

The coefficient c_0 follows from the result for ξ ($\xi = 0.475$ at NLO in the ϵ -expansion) using equ. (4). Matching equ. (18,19) against equ. (5,7) gives $c_2 = 0$ and $c_1/c_0 = 3/8 - \epsilon/4$. The corresponding energy density functional was studied in [10]. Compared to a free Fermi gas the local density term is reduced by a factor ~ 2 (the interaction is attractive), while the gradient correction proportional to $(\nabla n)^2/n$ is enhanced by a factor ~ 2 .

3. Transport Properties

In the following we will discuss transport properties of the Fermi gas at unitarity. The interest in non-equilibrium properties arises from the observation that transport coefficients are much more sensitive to the strength of the interaction than thermodynamic quantities. A renewed interest in transport properties was also sparked the AdS/CFT correspondence and the experimental limits on the shear viscosity of the quark gluon plasma obtained at RHIC. In the following we shall focus on the shear viscosity of the Fermi gas at unitarity. Close to equilibrium the (coarse grained) energy

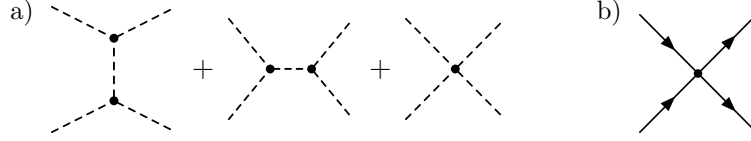


Fig. 4. Leading order processes that contribute to the shear viscosity at low temperature (Fig. a) and high temperature (Fig. b). Dashed lines are phonon propagators and solid lines are fermion propagators.

momentum tensor can be written as

$$T_{ij} = (P + \epsilon)v_i v_j - P\delta_{ij} + \delta T_{ij} , \quad (20)$$

$$\delta T_{ij} = -\eta(\nabla_i v_j + \nabla_j v_i - \frac{2}{3}\delta_{ij}\vec{\nabla} \cdot \vec{v}) + \dots ,$$

where ϵ and P are the energy density and pressure, and v_i is the local flow velocity. The first term is the ideal gas contribution, and δT_{ij} is the leading order (in gradients of v_i) dissipative correction. The traceless part of δT_{ij} is proportional to the shear viscosity η .

3.1. Kinetic Theory

We first consider the case that the fluid is composed of weakly interacting quasi-particles. In the unitarity limited Fermi gas this is the case at $T \ll T_c$ (phonons) and $T \gg T_c$ (atoms). In these limits we can compute the shear viscosity using kinetic theory. In the following we will concentrate on the low temperature case discussed in [15]. In kinetic theory the stress-energy tensor is given by

$$T_{ij} = v_s^2 \int \frac{d^3 p}{(2\pi)^3} \frac{p_i p_j}{E_p} f_p , \quad (21)$$

where f_p is the distribution function of the phonons, v_s is the speed of sound, p_i is the momentum and E_p the quasi-particle energy. Close to equilibrium $f_p = f_p^{(0)} + \delta f_p$, where $f_p^{(0)}$ is the Bose-Einstein distribution and δf_p is a small departure from equilibrium. We write $\delta f_p = -\chi(p)f_p^{(0)}(1 + f_p^{(0)})/T$. In the case of shear viscosity we can further decompose

$$\chi(p) = g(p)(p_i p_j - \frac{1}{3}\delta_{ij}p^2)(\nabla_i v_j + \nabla_j v_i - \frac{2}{3}\delta_{ij}\vec{\nabla} \cdot \vec{v}) . \quad (22)$$

Inserting equ. (22) into equ. (21) we get

$$\eta = \frac{4v^2}{15T} \int \frac{d^3 p}{(2\pi)^3} \frac{p^4}{2E_p} f_p^{(0)}(1 + f_p^{(0)})g(p) . \quad (23)$$

The non-equilibrium distribution $g(p)$ is determined by the Boltzmann equation

$$\frac{df_p}{dt} = \frac{\partial f_p}{\partial t} + \vec{v} \cdot \vec{\nabla} f_p = C[f_p], \quad (24)$$

relating the rate of change of the distribution function f_p to the collision operator $C[f_p]$. The $2 \leftrightarrow 2$ collision integral is given by

$$C_{2 \leftrightarrow 2}[f_p] = \frac{1}{2E_p} \int \frac{d^3k}{(2\pi)^3 2E_k} \frac{d^3k'}{(2\pi)^3 2E_{k'}} \frac{d^3p'}{(2\pi)^3 2E_{p'}} \times (2\pi)^4 \delta^{(4)}(p+k-p'-k') |\mathcal{M}|^2 D_{2 \leftrightarrow 2}, \quad (25)$$

where $D_{2 \leftrightarrow 2}$ contains the distribution functions and $|\mathcal{M}|$ is the $2 \leftrightarrow 2$ scattering amplitude shown in Fig. 4. The three and four-phonon vertices are fixed by the effective lagrangian (2). Linearizing $D_{2 \leftrightarrow 2}$ in δf_p one finds

$$D_{2 \leftrightarrow 2} = \frac{1}{T} f_{k'}^{(0)} f_{p'}^{(0)} (1 + f_k^{(0)}) (1 + f_p^{(0)}) (\chi(p) + \chi(k) - \chi(p') - \chi(k')). \quad (26)$$

There are a variety of methods for solving the linearized Boltzmann equation. A standard technique is based on expanding $g(p)$ in a complete set of functions. A nice feature of this method is that the truncated expansion gives a variational estimate

$$\eta \geq \frac{4v^4}{25T^2} \frac{(b_0 A_{00})^2}{\sum_{s,t} b_s b_t M_{st}} \quad (27)$$

where b_s is a set of expansion coefficients, A_{00} is a normalization integral, and M_{st} are matrix elements of the linearized collision operator. For the best trial function we find [15]

$$\eta/s = 7.7 \times 10^{-6} \xi^5 \frac{T_F^8}{T^8}, \quad (28)$$

where ξ is the universal parameter introduced in Sect. 2.1 and we have normalized the result to the entropy density s of a weakly interacting phonon gas. A similar estimate can be obtained in the high temperature limit. In this case the relevant degrees of freedom are atoms, and the dominant scattering process is shown in Fig. 4b. The result is [16,17]

$$\eta/s = \frac{45\pi^{3/2}}{64\sqrt{2}} \left(\frac{T}{T_F} \right)^{3/2} \left[\log \left(\frac{3\sqrt{\pi}}{4} \frac{T^{3/2}}{T_F^{3/2}} \right) + \frac{5}{2} \right]^{-1}. \quad (29)$$

The high and low temperature limits of η/s are shown in Fig. 5, together with the proposed lower bound $\eta/s = 1/(4\pi)$ [18] and experimental data which we will discuss in the next section.

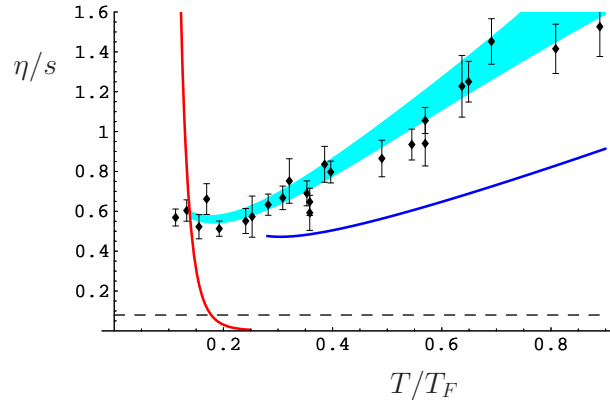


Fig. 5. Viscosity to entropy density ratio of a cold atomic gas in the unitarity limit. This plot is based on the damping data published in [8] and the thermodynamic data in [19,20]. The dashed line shows the conjectured viscosity bound $\eta/s = 1/(4\pi)$, and the solid lines show the high and low temperature limits.

3.2. Hydrodynamics

Hydrodynamics describes the evolution of long-wavelength, slow-frequency modes. The hydrodynamic description remains valid even if there is no underlying kinetic theory. The hydrodynamic equations follow from conservation of mass (particle number), energy and momentum. In a non-relativistic system the equations of continuity and of momentum conservation are given by

$$\frac{\partial n}{\partial t} + \vec{\nabla} \cdot (n\vec{v}) = 0, \quad (30)$$

$$mn \frac{\partial \vec{v}}{\partial t} + mn (\vec{v} \cdot \vec{\nabla}) \vec{v} = -\vec{\nabla} P - n \vec{\nabla} V, \quad (31)$$

where n is the number density, m is the mass of the atoms, \vec{v} is the fluid velocity, P is the pressure and V is the external potential. In an ideal fluid the equation of energy conservation can be rewritten as conservation of entropy,

$$\frac{\partial ns}{\partial t} + \vec{\nabla} \cdot (ns\vec{v}) = 0. \quad (32)$$

A non-zero shear viscosity leads to dissipation, converting kinetic energy to heat and increasing the entropy. The shear viscosity of the dilute Fermi gas in the unitarity limit can be measured by studying the damping of collective modes in trapped systems [21]. The frequency of these modes agrees well

the prediction of ideal hydrodynamics. The dissipated energy is given by

$$\dot{E} = -\frac{1}{2} \int d^3x \eta(x) \left(\partial_i v_j + \partial_j v_i - \frac{2}{3} \delta_{ij} \partial_k v_k \right)^2. \quad (33)$$

The damping rate is given by the ratio of the energy dissipated to the total energy of the collective mode. The kinetic energy is

$$E_{kin} = \frac{m}{2} \int d^3x n(x) \vec{v}^2. \quad (34)$$

If the damping rate is small both \dot{E} and E_{kin} can be computed using the solution of ideal hydrodynamics. We recently performed an analysis [22] which is based on measurements of the damping rate of the lowest radial breathing mode performed by the Duke group [8]. We showed that can relate the dimensionless ratio Γ/ω , where Γ is the damping rate and ω is the trap frequency, to the shear viscosity to entropy density ratio

$$\frac{\eta}{s} = \frac{3}{4} \xi^{1/2} (3N)^{1/3} \left(\frac{\bar{\omega}\Gamma}{\omega_{\perp}^2} \right) \left(\frac{E}{E_{T=0}} \right) \left(\frac{N}{S} \right). \quad (35)$$

Here N is the total number of particles in the trap ($2 \cdot 10^5$ in [8]), ξ is the universal parameter defined in Sec. 2.1, $E/E_{T=0}$ is the ratio of the total energy to the energy at $T = 0$ (which can be extracted using a Virial theorem from the measured cloud size), and S/N is the entropy per particle (which is measured using adiabatic sweeps to the BCS limit [20]). The results are compared to theoretical prediction in the high and low temperature limit in Fig. 5. The data show a minimum near $T/T_F \simeq 0.2$. At the minimum $\eta/s \sim 1/2$. This should probably be considered as an upper bound, since dissipative mechanism other than shear viscosity may be present. In the high T limit there is fairly good agreement with kinetic theory. The temperature dependence implied by the low T prediction is not seen in the data. This is maybe not very surprising, since the mean free path in the low T regime quickly exceeds the system size.

4. Outlook

There are many promising directions for further study. Clearly, it is desirable to obtain additional experimental constraints on the shear viscosity, and to improve the theoretical analysis of the existing data sets. It would also be interesting to confirm that the bulk viscosity vanishes in the normal phase, and to measure the thermal conductivity. We would also like to improve the theoretical tools for computing transport properties in the

interesting regime near T_c . There are some recent ideas for applying holography and the *AdS/CFT* correspondence to Galilean invariant conformal field theories [5,6], but there are also many purely field theoretic methods (ϵ expansions, large N methods) that have yet to be pursued.

Acknowledgments: Much of this work was carried out in collaboration with G. Rupak. The work is supported in part by the US Department of Energy grant DE-FG02-03ER41260.

References

1. E. Burovski, N. Prokof'ev, B. Svistunov, M. Troyer, Phys. Rev. Lett. **96**, 160402 (2006) [cond-mat/0602224].
2. A. Bulgac, J. E. Drut, P. Magierski, arXiv:0803.3238 [cond-mat.stat-mech].
3. M. G. Alford, A. Schmitt, K. Rajagopal and T. Schäfer, Rev. Mod. Phys., in press, arXiv:0709.4635 [hep-ph].
4. T. Mehen, I. W. Stewart and M. B. Wise, Phys. Lett. B **474**, 145 (2000) [arXiv:hep-th/9910025].
5. D. T. Son, arXiv:0804.3972 [hep-th].
6. K. Balasubramanian and J. McGreevy, arXiv:0804.4053 [hep-th].
7. K. M. O'Hara, S. L. Hemmer, M. E. Gehm, S. R. Granade, J. E. Thomas, Science **298**, 2179 (2002) [cond-mat/0212463].
8. J. Kinast, A. Turlapov, J. E. Thomas, Phys. Rev. Lett. **94**, 170404 (2005) [cond-mat/0502507].
9. D. T. Son and M. Wingate, Annals Phys. **321**, 197 (2006) [arXiv:cond-mat/0509786].
10. G. Rupak and T. Schäfer, arXiv:0804.2678 [nucl-th].
11. Z. Nussinov and S. Nussinov, Phys. Rev. A **74**, 053622 (2006), cond-mat/0410597.
12. Y. Nishida and D. T. Son, Phys. Rev. Lett. **97**, 050403 (2006) [arXiv:cond-mat/0604500].
13. Y. Nishida, Phys. Rev. A **75**, 063618 (2007) [arXiv:cond-mat/0608321].
14. A. Kryjevski, arXiv:0804.2919 [nucl-th].
15. G. Rupak and T. Schäfer, Phys. Rev. A **76**, 053607 (2007) [arXiv:0707.1520 [cond-mat.other]].
16. P. Massignan, G. M. Bruun, and H. Smith, Phys. Rev. A **71**, 033607 (2005).
17. G. M. Bruun and H. Smith, Phys. Rev. A **72**, 043605 (2005).
18. P. Kovtun, D. T. Son and A. O. Starinets, Phys. Rev. Lett. **94**, 111601 (2005) [hep-th/0405231].
19. J. Kinast, A. Turlapov, J. E. Thomas, Q. Chen, J. Stajic, and K. Levin, Science **307**, 1296 (2005) [cond-mat/0502087].
20. L. Luo, B. Clancy, J. Joseph, J. Kinast, J. E. Thomas, preprint, cond-mat/0611566.
21. J. Kinast, S. L. Hemmer, M. E. Gehm, A. Turlapov, and J. E. Thomas, Phys. Rev. Lett. **92**, 150402 (2004).
22. T. Schäfer, Phys. Rev. A **76**, 063618 (2007) [arXiv:cond-mat/0701251].